J. Fluid Mech. (1982), *vol.* 116, *pp.* 123–156
Printed in Great Britain

Experiments on the flow and acoustic properties of a moderate-Reynolds-number supersonic jet

By T. R. TROUTT† AND D. K. MCLAUGHLIN‡
Oklahoma State University, Stillwater, Oklahoma, USA

(Received 29 October 1979 and in revised form 21 July 1981)

An experimental investigation of the flow and acoustic properties of a moderate-Reynolds-number (Re = 70000), Mach number M = 2·1, axisymmetric jet has been performed. These measurements extended the experimental studies conducted previously in this laboratory to a higher-Reynolds-number regime where the flow and acoustic processes are considerably more complex. In fact, mean-flow and acoustic properties of this jet were determined to be closely comparable to published properties of high-Reynolds-number jets.

The major results of the flow-field measurements demonstrate that the jet shear annulus is unstable over a broad frequency range. The initial growth rates and wavelengths of these instabilities as measured by a hot wire were found to be in reasonable agreement with linear stability theory predictions. Also, in agreement with subsonic-jet results, the potential core of the jet was found to be most responsive to excitation at frequencies near a Strouhal number of S = 0·3. The overall development of organized disturbances around S = 0·2 seems to agree in general with calculations performed using the instability theory originally developed by Morris and Tam.

The acoustic near field was characterized in terms of sound-pressure level and directivity for both natural and excited (pure-tone) jets. In addition, propagation direction and azimuthal character of dominant spectral components were also measured. It was determined that the large-scale flow disturbances radiate noise in a directional pattern centred about 30° from the jet axis. The noise from these disturbances appears from simple ray tracing to be generated primarily near the region of the jet where the coherent fluctuations saturate in amplitude and begin to decay. It was also determined that the large-scale components of the near-field sound are made up predominately of axisymmetric (n = 0) and helical (n = ±1) modes. The dominant noise-generation mechanism appears to be a combination of Mach-wave generation and a process associated with the saturation and disintegration of the large-scale instability. Finally, the further development of a noise-generation model of the instability type appears to hold considerable promise.

1. Introduction

Experiments on low-Reynolds-number high-speed jets conducted previously in our laboratory by McLaughlin, Morrison & Troutt (1975, 1977) and Stromberg, McLaughlin & Troutt (1979) have shown that large-scale discrete instabilities

† Present address: Washington State University, Pullman, Washington.
‡ Present address: Dynamics Technology, Inc., Torrance, California.

dominate the flow fluctuations of these jets upstream of the end of the potential core. For the case of the supersonic jets ($M = 1{\cdot}3$ to $M = 2{\cdot}5$), these large-scale instabilities were determined to be *directly responsible* for a major portion of the noise radiated by the jets. This noise was found to have similar scaled amplitudes and directivity distributions as published results from high-Reynolds-number jets of equivalent Mach numbers (Dosanjh & Yu 1968; Yu & Dosanjh 1972). These results established experimentally the ability of large-scale flow instabilities to produce noise efficiently.

The potential of organized large-scale disturbances for producing noise was initially suggested by Mollo-Christensen (1960, 1967) with later contributions by Sedel'nikov (1967), Michalke (1969) and Bishop, Ffowcs Williams & Smith (1971). The existence of these large structures in low-speed jets has been demonstrated by a number of experimental studies, most notably Crow & Champagne (1971), Lau, Fisher & Fuchs (1972), and Chan (1974). However, for high-speed turbulent jets, direct flow measurements are difficult to obtain. Indirect observations using flow-visualization techniques (Lowson & Ollerhead 1968; Potter 1968; Salant 1973), however, have indicated the presence of large-scale wavelike disturbances in turbulent supersonic jets.

One of the first attempts to produce a mathematical representation of jet-noise generation by organized disturbances was presented by Tam (1972). Tam's model at that time used a linearized spatial-instability theory to develop an eigenvalue relation between the complex wavenumber and the frequency of the unstable wave. This instability theory followed the same general methods as were employed by Sedel'nikov (1967) and Michalke (1969). Since Tam's model assumed infinitesimally thin shear layers and a parallel mean flow, his results indicated that a monotonic increase in wave growth rate with increasing frequency would occur near the nozzle exit. In order to align his theoretical results with the large-scale structure observed in the downstream region of the jet, Tam imposed a selection mechanism on the instability results. Tam's hypothesized mechanism used the order induced on the supersonic jet by the wave-cell structure to accomplish this selection. However, recent evidence in low-Reynolds-number supersonic jets over a substantial Mach-number range obtained by Morrison & McLaughlin (1980) fail to support this mechanism.

Subsequent work on more advanced jet-instability and noise-prediction models has been performed by a number of investigators including Chan (1974), Tam (1975), Merkine & Liu (1975), Morris (1977) and Morris & Tam (1977). The primary concern of these works has been to develop more realistic flow models. Since acoustic measurements indicate that the dominant noise generation region is near the end of the potential core, nonlinear effects are no doubt important. The exact method of best incorporating these effects into mathematical models though is a controversial point. In the Morris & Tam (1977) theory nonlinear effects have been accounted for indirectly by using empirical mean-flow profiles as inputs to the local linear instability calculations. However, as was pointed out by Morris (1977), the actual importance of explicit nonlinear terms in the calculations is simply not known at the present time.

Certainly, the formulation of the nonlinear effects in the instability analysis is one of the major problems facing the researchers developing analytical jet-noise

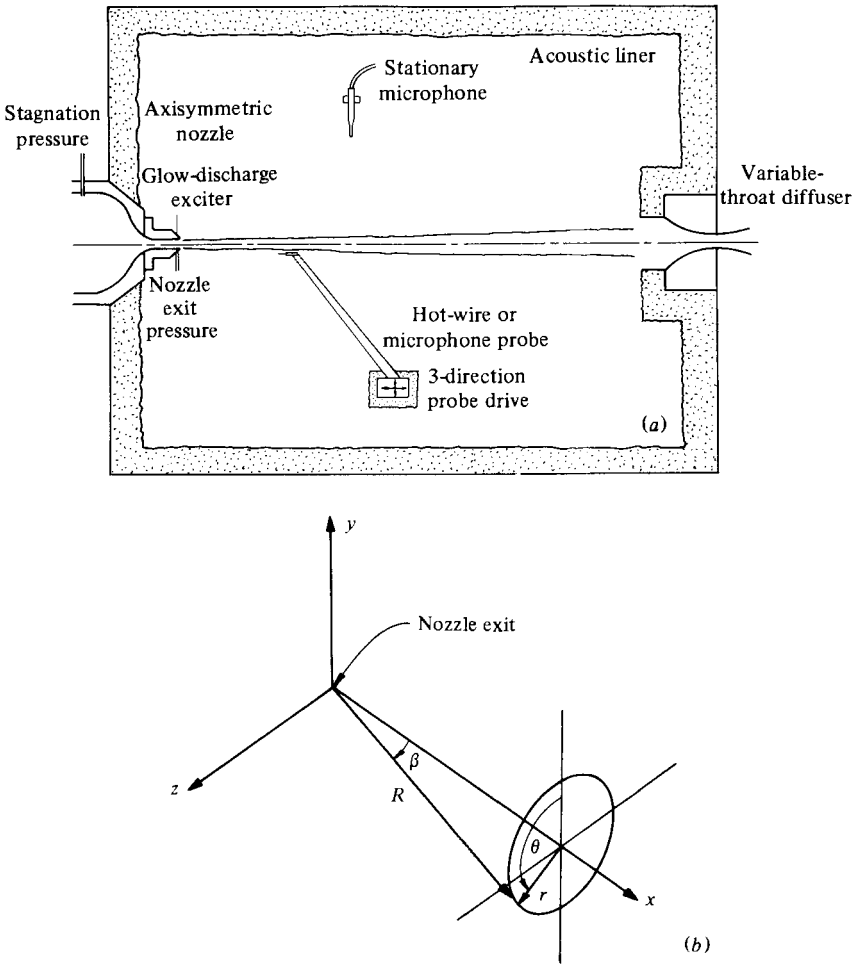

FIGURE 1. (*a*) Schematic diagram of the jet test chamber. (*b*) Co-ordinate system.

models. Another major problem is the effect of non-parallel flow (flow divergence). For an incompressible jet, Crighton & Gaster (1976) have developed a method incorporating the flow-divergence effects. In the supersonic jet, Morris & Tam (1977) have performed a similar analysis; however, the exact accuracy of some of their acoustic field calculations is suspect (Morris & Tam 1979 private communication).

No doubt the progress of the theoretical models could be aided greatly by experimental studies on the coherent structures in turbulent high-speed jets, but involved flow measurements in supersonic jets are difficult to make. The most reliable turbulence instrument, the hot-wire anemometer, cannot be used in conventional high-speed air jets because the dynamic pressures are too great for the fragile probes. This problem can be alleviated by reducing the density of the flow; a practice followed in the earlier work, mentioned previously, conducted in our laboratory. At the low Reynolds numbers of these measurements, the flow fluctuations of the supersonic jets were found to be dominated by discrete large-scale instabilities for approximately the entire length of the potential core. And as mentioned earlier

the low-Reynolds-number experiments were important in establishing the noise-radiation potential of the large-scale instability waves in the jet.

In order to achieve an experimental condition more closely approaching a high-Reynolds-number jet the present study was carried out at a Reynolds number of $Re = 70000$, which is approximately 10 times greater than that of the previous low-Re studies. This moderate Reynolds number was chosen as a compromise between the increasingly more difficult experimental conditions and the increasingly more interesting and more involved flow and acoustic phenomena encountered at higher Reynolds numbers. At the chosen Reynolds number, both the flow and acoustic properties were found to be considerably more complex than the low-Reynolds-number jets. In fact, based on comparisons of mean-flow and acoustic results presented here with high-Reynolds-number measurements, considerable support can be found for extrapolating many of the present results to high Re.

The goal of the present research was to characterize experimentally the dominant flow-fluctuation properties in a $M = 2{\cdot}1$ moderate-Reynolds-number jet, and to investigate the related noise-generation process. The experiments included measurements on both natural and artificially excited jets. The artificially excited measurements were used to illuminate properties of the coherent-flow structure and its radiated noise.

2. Experimental apparatus and procedures

2.1. *Apparatus*

These experiments were conducted in the free jet test facility shown schematically in figure 1. This facility has been described in a previous reference (McLaughlin *et al.* 1977), so that only a brief description will be given here.

An axisymmetric supersonic nozzle with an exit diameter D of 10 mm was used to produce the air jet. The nozzle contour was designed by the method of characteristics, following Johnson & Boney (1975). The nominal $M = 2$ air jet exhausts into a low-pressure test chamber of dimensions $1{\cdot}1 \times 0{\cdot}76 \times 0{\cdot}71$ m. The chamber is lined with acoustic foam, which absorbs over 90 % of the incident radiation for frequencies f above 1 kHz. (The characteristic frequency of the jet is $U_0/D = 50$ kHz, where U_0 is the jet exit velocity.)

A three-dimensional probe-drive system was used to position the Pitot pressure, hot-wire and microphone probes employed in the research. The Pitot probe was a standard blunt-end type with an outside diameter of 0·53 mm. The hot-wire probes used were DISA 55A53 subminiature probes mounted on brass wedges. The 5 μm diameter wires were positioned perpendicular to the axial direction. DISA 55M constant-temperature electronics were used to operate the probes. The frequency response of the anemometer was found to be flat within ± 3 dB up to 60 kHz ($S = fD/U_0 = 1{\cdot}2$) based on square-wave-response tests. A Bruel & Kjaer 3·18 mm diameter condenser microphone was used for the acoustic measurements. The microphone was assumed to have an omnidirectional response for frequencies up to 80 kHz, based on factory specifications. For overall level measurements both the microphones and hot-wire signals were band-pass filtered from $S = 0{\cdot}03$ to $S = 1{\cdot}3$ to remove chamber and electronic resonances. Frequency spectra of the sensor signals were obtained using a Tektronix 7L5 analyser. For the spectra

presented from the present measurements, a resolution window of either 300 Hz or 3 kHz was used.

The jet was artificially excited for some measurements using a glow-discharge device consisting of a single-point tungsten electrode positioned approximately 2 mm from the nozzle exit (McLaughlin *et al.* 1975).

2.2. *Procedures*

For all measurements in this study, the stagnation temperature of the jet was room temperature, approximately 294 K, and the jet-exit pressure p_e was maintained slightly above the test-chamber pressure p_c (approximately $1{\cdot}03p_c$). The test-chamber pressure for these measurements was approximately 0·05 atm and the Reynolds number based on exit conditions was approximately 70000.

Correlations and phase averages of sensor signals were measured using a Saicor 43A analyser. The phase average of a fluctuating signal is defined here as

$$\langle q(t)\rangle = \lim_{N\to\infty} \frac{1}{N} \sum_{n=0}^{N} q(t+n\tau),$$

where τ is the period of the coherent disturbance, N is the number of disturbance cycles averaged over, and t is time. The application of this function allows the recovery of the periodic portion of the fluctuating signal where a general representation of the signal is given by

$$q(t) = \bar{q} + \tilde{q}(t) + q''(t).$$

Here $\bar{q}$ is the mean component, with the fluctuating component divided into two parts: the period portion $\tilde{q}$, and the random contribution q''.

For flow-fluctuation-amplitude measurements, the hot-wire bridge-voltage fluctuation e' is related to the fluctuation in the flow quantity axial mass velocity ρu by the relation $e'/\bar{e} = Am(\overline{u\rho})'/\rho u$ where the sensitivity coefficient Am was determined through direct calibration following the methods of Rose (1973) and Ko, McLaughlin & Troutt (1978). The above relation is applicable when total temperature fluctuations are assumed negligible. For the present measurements the total temperature fluctuations were found to account for less than 2 % of the voltage fluctuation.

Sound pressure levels (in dB) were scaled to the ambient test-chamber pressure using the relation

$$\mathrm{SPL} = 20 \log_{10}[p'_{\mathrm{rms}}/(p_c p_{\mathrm{ref}}/p_a)],$$

where p'_{rms} is the root mean square of the fluctuating sound pressure, p_a is standard atmospheric pressure and $p_{\mathrm{ref}} = 2\times10^{-5}$ N/m^2.

3. Experimental results

3.1. *Natural jet*

3.1.1. *Mean-flow field.* The centre-line Mach-number distribution for the present Re = 70000 jet is shown in figure 2. The Mach number is calculated from Pitot- and static-pressure-probe measurements using standard compressible-flow relationships. The average centre-line Mach number from $x/D = 1$ to $x/D = 8$ was found to be 2·12, with variations of ± 4 % due to the weak shock-cell structure of the jet. These measurements indicate the potential-core length of the jet to be between

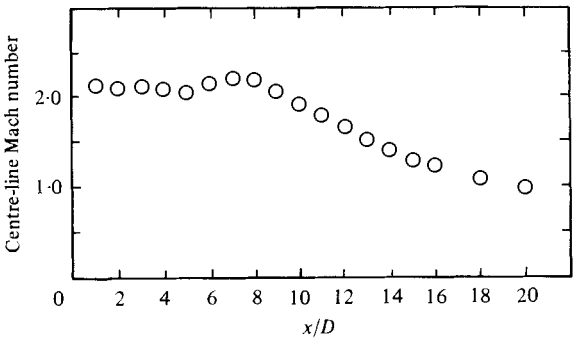

FIGURE 2. Distribution of mean Mach number on the jet centre line.

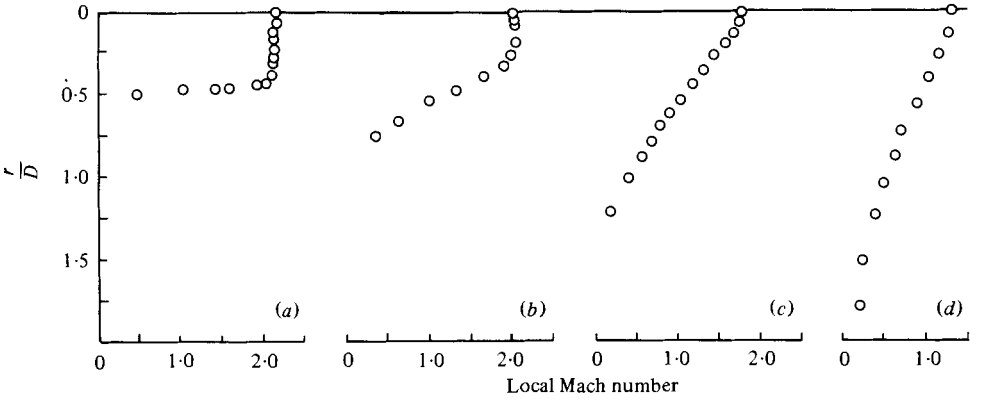

FIGURE 3. Radial Mach-number profiles. x/D: (*a*) 1; (*b*) 5; (*c*) 10; (*d*) 15.

8 and 10 diameters. The sonic point in the jet is reached between 18 and 20 diameters downstream of the nozzle exit. Radial Mach-number profiles for $x/D = 1$, 5, 10 and 15 are shown in figure 3. These measurements show that the mean flow changes from a profile with a central region of uniform velocity to an approximately Gaussian profile by $x/D = 10$.

The centre-line Mach-number distribution and the Mach-number profiles are similar to the data obtained by Dutt (1977) and by McLaughlin, Seiner & Liu (1980) for cold-air jets of Mach number 2·0 and Reynolds numbers in excess of $Re = 10^6$. However, a more careful look at the shear-layer development yields some differences. To do this we have used a curve fit for the velocity profiles similar to the one used by Laufer, Kaplun & Chu (1973) for subsonic jets. It takes the form of a half-Gaussian

$$\tilde{u}(\eta) = \begin{cases} \exp\left[-2{\cdot}773(\eta+0{\cdot}5)^2\right] & \text{for} \quad \eta > -0{\cdot}5, \\ 1 & \text{for} \quad \eta \leqslant -0{\cdot}5, \end{cases}$$

where $\eta = (r - r(0{\cdot}5))/\delta$, U is the velocity on the centre line of the jet at the given axial (x) location, $r(0{\cdot}5)$ is the radial location where the velocity is $0{\cdot}5U$, and δ is the local shear-layer thickness. Downstream of the end of the potential core $\delta = 2r(0{\cdot}5)$ and η reduces to $\eta = r/\delta - \frac{1}{2}$, where δ is now $\frac{1}{2}$ the local jet diameter. (The jet diameter is taken to be the diameter of the locus of points where the mean velocity is 0·01 times the local centre-line velocity.) Morris & Tam (1977) have also

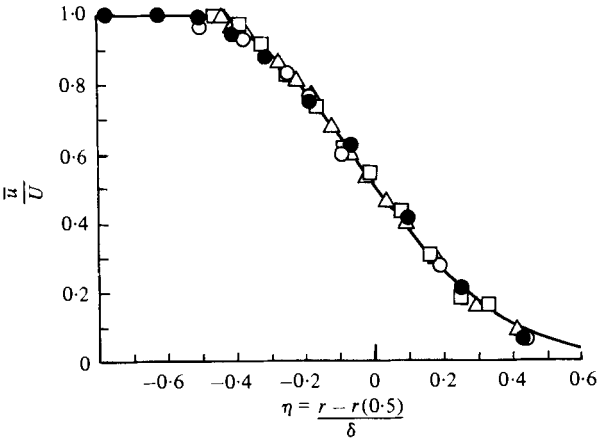

FIGURE 4. Mean-velocity data. x/D: ○, 1; ●, 5; △, 10; □, 15.

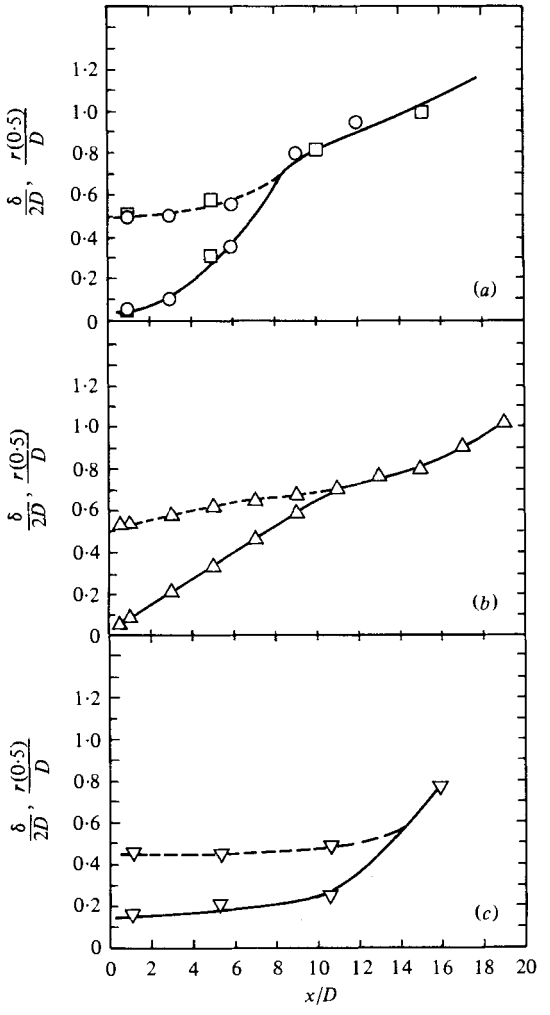

FIGURE 5. Axial distribution of mean-velocity-profile parameters. (*a*) $M = 2{\cdot}1$, $Re = 70000$; (*b*) $M = 2{\cdot}0$, $Re = 5{\cdot}2 \times 10^6$; (*c*) $M = 2{\cdot}1$, $Re = 7900$. ——, $\delta/2D$; · · ·, $r(0{\cdot}5)/D$.

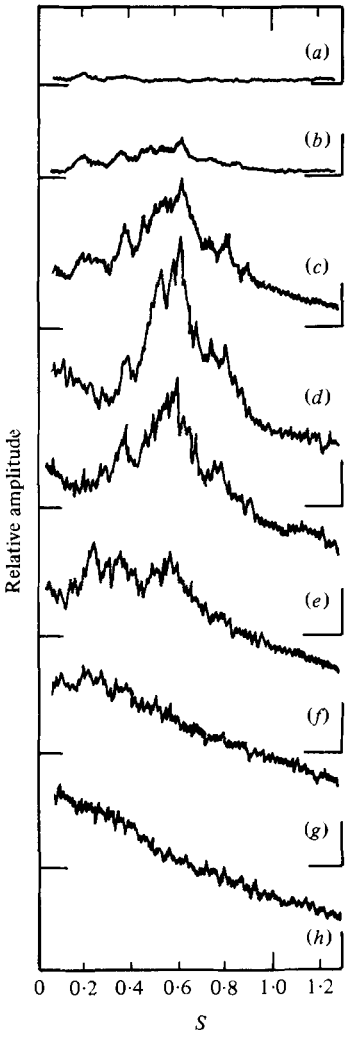

FIGURE 6. Hot-wire spectra at several axial locations in the jet shear layer. x/D: (*a*) 1; (*b*) 2; (*c*) 3; (*d*) 4; (*e*) 5; (*f*) 6; (*g*) 8; (*h*) 10.

shown the above half-Gaussian to be a convenient curve fit for supersonic-jet velocity data, particularly for input into the instability analysis of the jet.

Figure 4 includes mean-velocity data of the four axial locations corresponding to the Mach-number data of figure 3. This figure demonstrates that the half-Gaussian is a reasonable representation for the mean-velocity data both upstream and downstream of the end of the potential core. The local shear-layer thickness δ and the $r(0{\cdot}5)$ parameter used to generate the best curve fits are plotted in figure 5 as functions of the axial co-ordinate. Included on the figure are the data for the same parameters determined by measurements made by McLaughlin *et al.* (1980) in a Mach number 2·0, $Re = 5{\cdot}2 \times 10^6$ jet. There is a reasonable similarity in the development of the present moderate-Reynolds-number jet in comparison with its high-Reynolds-number counterpart. However, the shear layer in the potential-core region of the jet does not display the linear growth dependence typical of fully

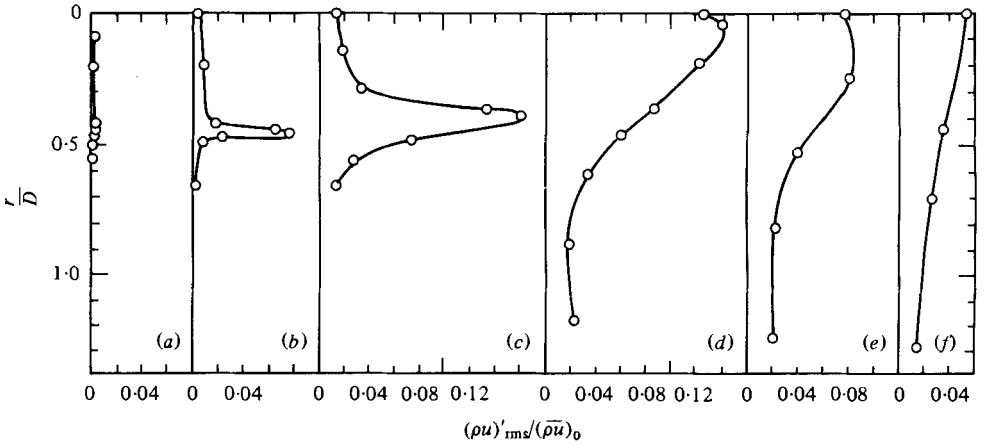

FIGURE 7. Radial profiles of mass-velocity fluctuation amplitude. x/D: (*a*) 1; (*b*) 3; (*c*) 6; (*d*) 9; (*e*) 12; (*f*) 15.

turbulent shear layers. This slow initial growth rate indicates that the jet shear layer is in transition from laminar to turbulent flow in the moderate-Reynolds-number jet. Hot-wire measurements presented subsequently demonstrate that the laminar to turbulent transition in the shear layer occurs over the first 2 or 3 jet diameters. This contrasts to the extensive length of transitional flow found in the low-Reynolds-number (Re = 7900) jet as measured by Morrison & McLaughlin (1980). The low-Reynolds-number jet parameters are also shown in figure 5 for comparison.

3.1.2. *Fluctuating-flow field.* Frequency spectra of the hot-wire fluctuation signal obtained at the radial position of maximum voltage fluctuation (which is approximately the centre of the jet shear layer) are shown in figure 6 for several x/D locations. Beyond x/D = 8 the probe was located on the centre line of the jet. These spectra show that high-frequency flow fluctuations centred around a Strouhal number of approximately 0·6 grow rapidly and dominate the spectra for the first three diameters downstream of the jet exit. At x/D = 4, although the high-frequency fluctuations still dominate the spectra, a marked increase in the amplitude of low frequencies (below S = 0·25) can be seen. From x/D = 4 to x/D = 6 the high-frequency fluctuations decay steadily, transferring energy into intermediate frequencies around S = 0·30.

Spectral-energy transfer to intermediate frequencies continues from x/D = 6 to x/D = 8, resulting in a fully developed turbulent spectrum at x/D = 8. Beyond x/D = 8, the fluctuation spectra shift continuously towards lower-frequency content with downstream location as indicated by the spectrum at x/D = 10. The general shape and development of these spectra is quite similar to spectra measured by Miksad (1972) in an incompressible free-shear layer. However, the spectra differ considerably from the low-Reynolds-number supersonic-jet spectra (Morrison & McLaughlin 1980) which were found to be dominated by a narrow frequency band near S = 0·2 for the first 10 jet diameters.

Figure 7 shows radial profiles of the mass-velocity fluctuations in the jet for several downstream positions. The measurements are reported in terms of r.m.s. mass-velocity fluctuations $(\rho u)'_{\mathrm{rms}}$, non-dimensionalized by the mean mass velocity

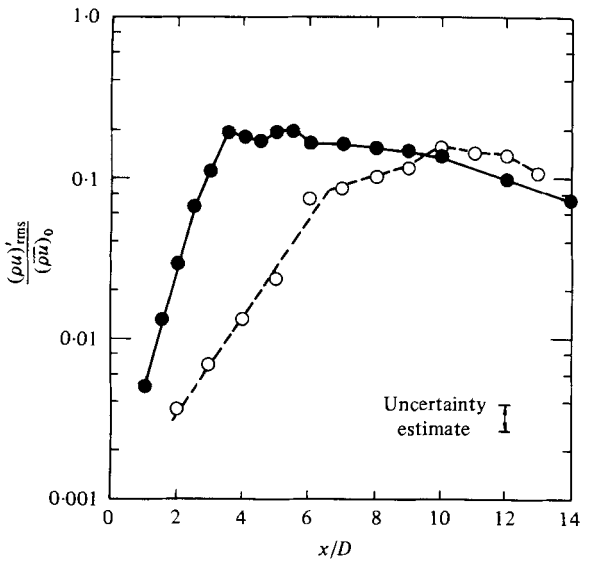

FIGURE 8. Overall mass-velocity fluctuation amplitude in the jet shear layer. *Re*: ●, 70000; ○, 7900; Morrison (1977).

at the centre line of the nozzle exit, $(\overline{\rho u})_0$. The radial peak of the fluctuation amplitude moves toward the centre of the jet, and the width of the shear layer increases with downstream location. By $x/D = 9$ it is apparent that large-amplitude fluctuations have reached the jet centre line, indicating the end of the potential-core region. This result is consistent with the mean-flow measurements, which showed a decrease in Mach number beginning in this region.

Flow fluctuation-amplitude measurements as functions of x/D are shown in figure 8. Prior to the end of the potential core these measurements were obtained with the hot-wire located in the centre of the shear layer. After the end of the potential core the hot wire was positioned on the jet centre line. The measurements show that the amplitude of the fluctuations grows approximately exponentially for the first 3 downstream diameters.' The amplitude of the fluctuations then oscillates from $x/D = 4$ to $x/D = 7$ before beginning a steady decline at $x/D = 8$. Also shown in the figure for comparison are measurements obtained by Morrison & McLaughlin (1980) in the low-Reynolds-number jet. Associated with the increasing Reynolds number is an increase in the growth rate of the fluctuations, accompanied by an upstream shift in the location of maximum fluctuation level in the jet. The upstream shift is consistent with the faster development of the mean-flow profiles, as illustrated earlier in figure 5.

In a hydrodynamic-instability theory the mathematical representation for any fluctuating flow property can be given by

$$q(x, r, \theta, t) = \hat{q}(r) \exp\left[-k_{\rm i} x + i\,(k_{\rm r} x + n\theta - \omega t)\right].$$

For a parallel-flow, $M = 2{\cdot}0$ jet with an infinitesimally thin shear annulus Tam (1972) has predicted the axial growth rate $k_{\rm i}$ as a function of frequency ω. To compare with Tam's theory, band-passed $(\rho u)'_{\rm rms}$ amplitude measurements were made at several Strouhal numbers in the region of initial exponential growth. The

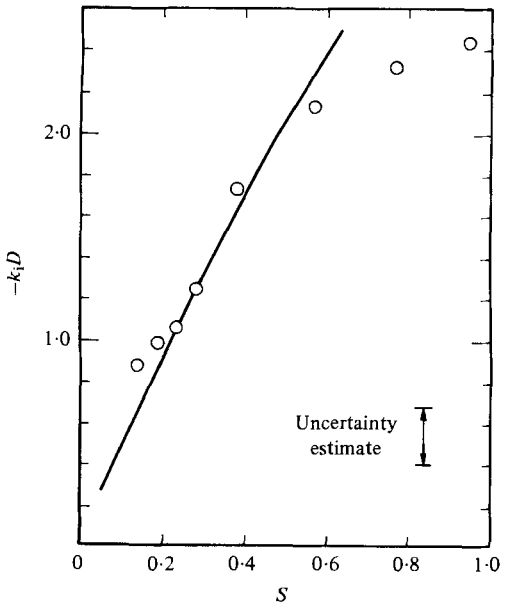

FIGURE 9. Initial mass-velocity fluctuation growth rates.
○, present experiments; ——, Tam (1972) prediction.

growth rates calculated from these measurements and Tam's prediction are shown in figure 9. Below $S = 0{\cdot}14$ no data were plotted because no significant length of constant exponential growth could be found at these low frequencies. There is excellent agreement between experiment and prediction for Strouhal numbers up to $S = 0{\cdot}6$. Above this frequency the instability analysis using the unrealistic top-hat mean-velocity profile predicts a constant increase in the growth rates (with frequency) while measurements indicate a levelling off of the growth rate. Presumably the initial growth rates will eventually begin to drop at higher frequencies in a manner similar to the predictions of Michalke (1971) for lower-Mach-number jets. However, these higher frequencies are beyond the capability of our instrumentation.

Tam's analysis assumes an $n = \pm 1$ azimuthal mode shape for the instability. This assumption seemed reasonable based on visualizations of axisymmetric supersonic jets (see Tam 1972). The question of the azimuthal-mode content for the present situation is addressed in §3.2.

Figure 10 shows the downstream development of two important spectral components of the mass-velocity fluctuations $(\rho u)'_{\mathrm{rms}}$. These data are normalized with the fluctuating value at $x/D = 1$, and the spectral components were chosen because of the importance of these frequencies in the noise-radiation field (see §3.1.3). To facilitate comparison with theoretical instability predictions these particular measurements were made at a constant radial position, $r/D = 0{\cdot}5$. McLaughlin *et al.* (1980) have performed the instability calculations for this jet flow using the Morris–Tam method documented with a computer code in Tester *et al.* (1978). The predictions for both the $n = 0$ and $n = 1$ modes are included in figure 10, where the calculation has been matched to the experimental values at the $x/D = 1$, initial condition. The mean-velocity profiles input into the calculation are the half-Gaussians discussed in §3.1.1, with the parameters given in figure 5(*a*).

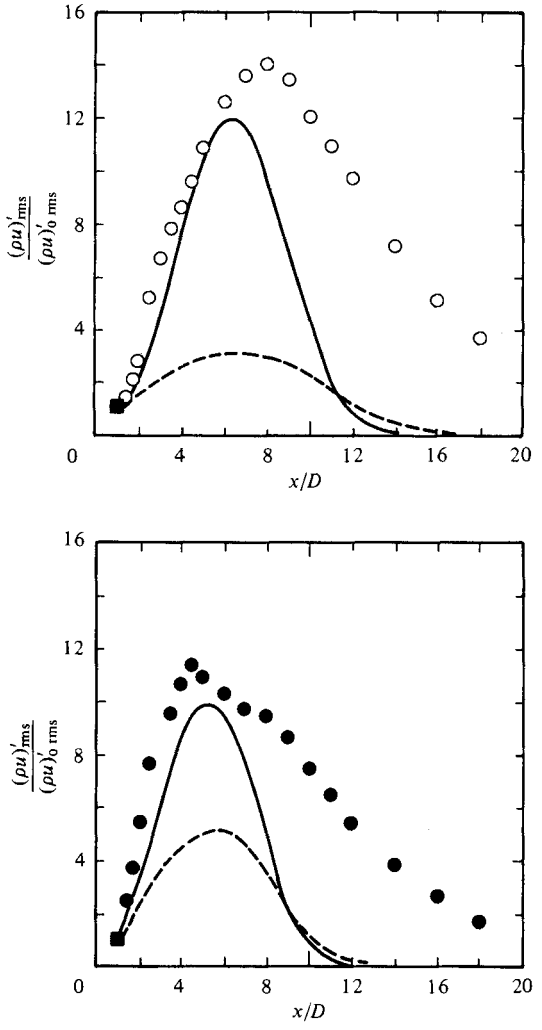

FIGURE 10. Band-passed mass-velocity fluctuation level in the jet shear layer. Present experiments: S: ○, 0·2; ●, 0·4. Tester *et al.* (1978) prediction: ——, $n = 1$; - - -, $n = 0$.

It is apparent that the instability calculation does a reasonable job of predicting the axial location of peak amplitude of each spectral component. The decay portion of the wave evolution is obviously poorly represented by the calculation. However, in the band-passed data, fluctuations which are not coherent with the upstream wave system are included in the measurement whereas the authors of the instability theory (Morris & Tam 1977) believe the calculation only represents the coherent portion. This point will be addressed directly in §3.2 of this paper.

3.1.3. *Acoustic field.* Sound-pressure level (SPL) contours of the overall near-field noise are shown in figure 11. The near-field contours are similar to high-Reynolds-number measurements in amplitude levels and general shape (Yu & Dosanjh 1972; McLaughlin *et al.* 1980). The contours are also similar in shape and amplitude to the noise contours Morrison & McLaughlin (1979) measured for the low-Reynolds-number jet at the same Mach number. (The low-Reynolds-number contours are

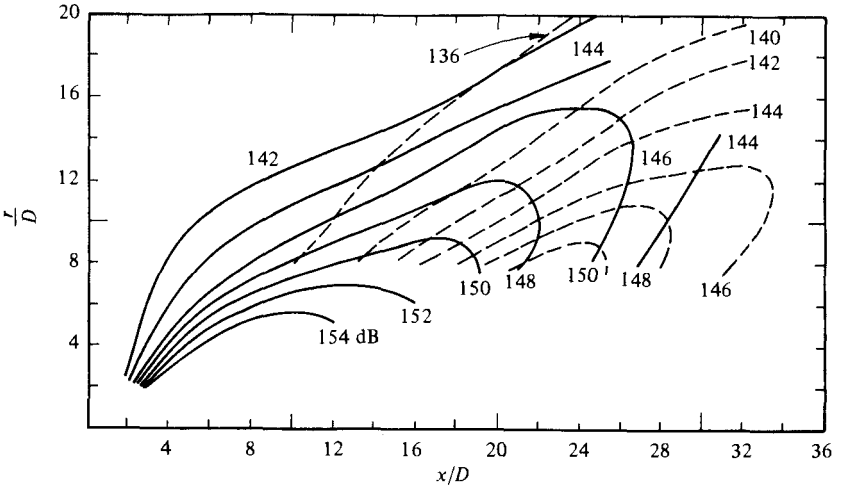

FIGURE 11. Overall sound-pressure level contours. ——, Re = 70000; - - -, Re = 7900; Morrison & McLaughlin (1979).

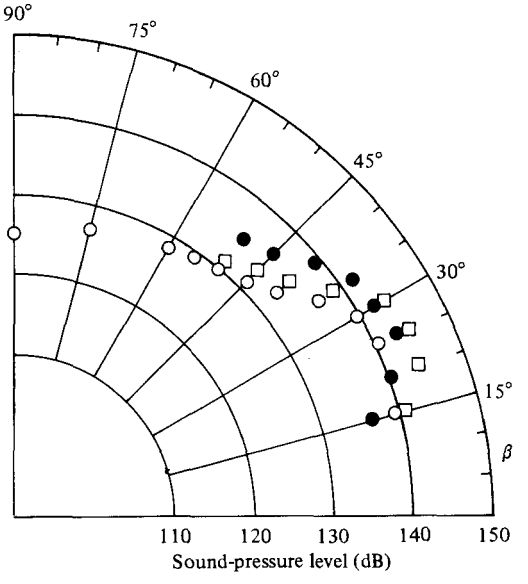

FIGURE 12. Directivity plot of overall sound-pressure level, R/D = 40. □, M = 2·1, Re = 7900; ●, M = 2·1, Re = 70000, ○, M = 2·0, Re = 5·2 × 10^6.

shown in dashed lines on the figure.) However, one important difference between the low-Reynolds-number results and the present measurements is obvious. The low-Reynolds-number contours are displaced downstream 6 to 10 jet diameters from the high-Reynolds-number contours. This displacement is most probably related to the fact that the amplitude of the flow fluctuations saturates farther downstream in the low-Reynolds-number jet, as we saw in figure 8.

Figure 12 shows the sound-pressure level as a function of the angle from the jet axis. These measurements were made at a constant polar radius of 40 jet diameters from the nozzle exit. Also shown on the figure are comparison data from a M = 2·0 jet at a high Reynolds number obtained by McLaughlin *et al.* (1980) and low-

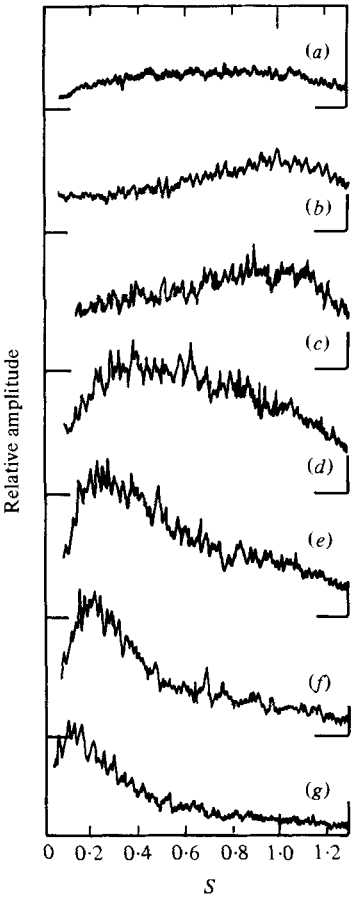

FIGURE 13. Microphone spectra, $r/D = 8$. x/D: (*a*) 4; (*b*) 8; (*c*) 12; (*d*) 16; (*e*) 20; (*f*) 24; (*g*) 28.

Reynolds-number data from Morrison & McLaughlin (1979). This figure shows that for all jets shown the highest levels of generated noise occur at angles around 30° to the jet axis.

In supersonic jets, particularly where the Mach number is 2 or larger, the major portion of the field surveyed in figures 11 and 12 is a radiating field. Only within about 4 or 5 diameters of the jet axis are there any significant hydrodynamic fluctuations. Phase-front data recorded by Morrison & McLaughlin (1979) show this to be the case. Consequently, except for a minor correction associated with the centroid of the noise source region being about 8 jet diameters downstream, the data presented in figure 12 provide a reasonable representation of the far-field directivity.

Spectral analyses of the microphone signal obtained at several locations along a constant radial co-ordinate are presented in figure 13. These spectra show a shift towards increased lower-frequency content as downstream position is increased. This trend has been noted in high-Reynolds-number jet-noise measurements by previous investigators (Yu & Dosanjh 1972; Laufer, Schlinker & Kaplan 1976). This trend is also in general agreement with hot-wire spectral results mentioned earlier.

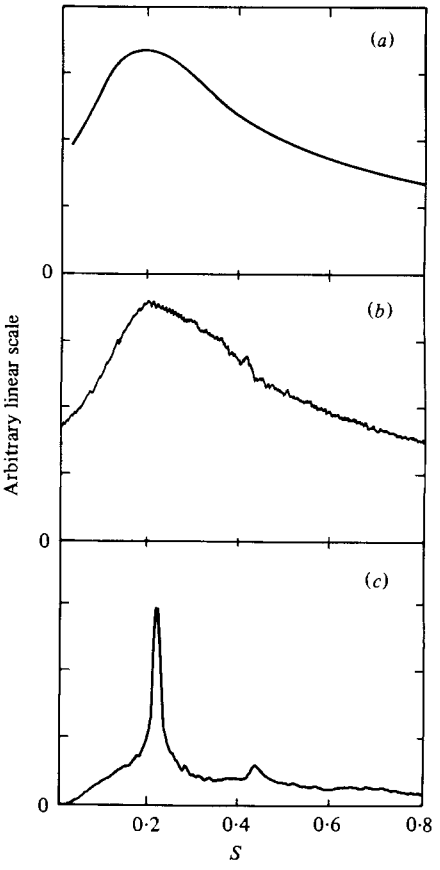

FIGURE 14. Acoustic spectra in the major noise-emission direction. (*a*) $M = 2{\cdot}0$, $Re = 2{\cdot}6 \times 10^6$; (*b*) $M = 2{\cdot}1$, $Re = 70000$; (*c*) $M = 2{\cdot}1$, $Re = 7900$.

To demonstrate the effect of Reynolds number on the acoustic frequency content, spectra from three different jets are presented in figure 14. These spectra were measured near the angle of maximum noise emission of the three jets. The bottom spectrum is from the low-Reynolds-number jet measured by Morrison & McLaughlin (1979), the middle spectrum is from the present measurements, and the top spectrum was reported by Laufer *et al.* (1976) for a $Re = 2{\cdot}6 \times 10^6$, $M = 2{\cdot}0$ jet. At the low-Reynolds-number condition, the flow is dominated by a narrow band of frequencies and the noise spectrum is similar. At the two higher-Reynolds-number conditions, the spectra are quite full; however, both have a broad peak around $S = 0{\cdot}2$ that coincides approximately with the low-Reynolds-number peak.

SPL contours of the near-field noise band-passed around two different spectral components ($S = 0{\cdot}2$ and $S = 0{\cdot}4$) are shown in figure 15. These frequencies encompass a large portion of the broad peak of the dominant noise spectrum. Two important general features of these contours should be noted. One is the presence of downstream lobes, which are apparent at both frequencies. The other feature is a bulge located in the upstream region of the contours. This upstream bulge is barely apparent in the higher-Strouhal-number contours, but becomes more obvious in the lower-Strouhal-number plot. For the lower-Strouhal-number contours, a

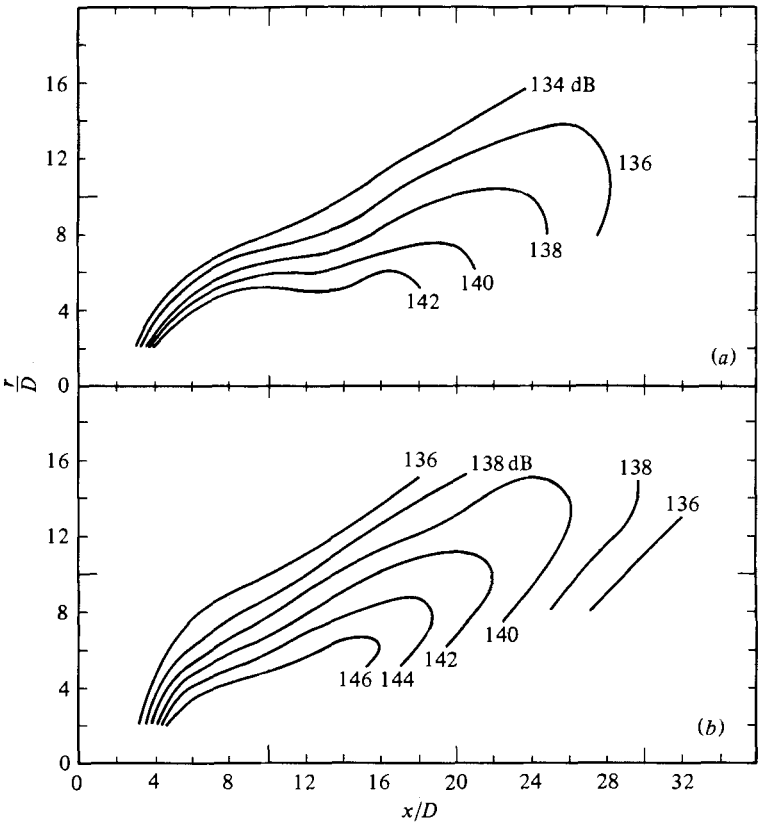

FIGURE 15. Band-passed sound-pressure level contours. (*a*) S = 0·15–0·23, (*b*) S = 0·30–0·45.

definite separation between the two regions is evident. These two regions have been noticed before by previous investigators (Laufer *et al.* 1976; Yu & Dosanjh 1972).

3.1.4. *Summary of natural-jet results.* The mean-flow measurements show that the jet has an initial central region of uniform velocity, which transitions to an approximately Gaussian profile by x/D = 10. The average Mach number of the jet was found to be 2·12 in the potential-core region, and the sonic point was reached between 18 and 20 diameters downstream. These mean-flow results are similar to high-Reynolds-number measurements at equivalent Mach numbers.

A more quantitative measure of the mean flow development was obtained by plotting δ, the local shear-layer thickness, as a function of the axial co-ordinate x. This plot showed that the moderate-Reynolds-number jet developed somewhat slower initially than high-Reynolds-number jets. This difference was attributed to the initial region of transitional flow near the nozzle exit.

Flow-fluctuation measurements indicate that frequencies from around S = 0·14 upward grow initially at constant exponential rates. These initial growth rates as a function of Strouhal number are predicted quite well by Tam's (1972) theory over the published range of the theoretical results. Beyond x/D = 3 nonlinear effects become apparent, and by x/D = 5 the flow-fluctuation spectra are quite broad and the overall fluctuation amplitude attains a saturated condition. By

$x/D = 8$ the spectra are fully developed. Beyond $x/D = 8$ the amplitude of the flow fluctuations decreases, and the spectral content of the fluctuations shifts progressively to lower frequencies.

Prediction of individual band-passed spectral components downstream of the saturation region using the Morris–Tam instability analysis and measured mean-velocity profiles had marginal success. The axial location of the peak fluctuation level is quite well predicted but the decay rates are poorly represented. However, this part of the analysis has better success in the artificially excited jet case discussed in §3.2 of this paper.

The present results differ considerably from low-Reynolds-number measurements at the same Mach number. The lower-Reynolds-number fluctuations were found by Morrison (1977) to be dominated by a narrow band of frequencies near $S = 0{\cdot}2$ for the first 10 diameters downstream of the jet exit. Growth rates of the flow fluctuations in the low-Reynolds-number jet are much slower, and the fluctuation level does not saturate until $x/D = 10$.

Acoustic spectra demonstrate that the noise produced by the moderate-Reynolds-number jet has a broad frequency content. The content of the acoustic spectra was observed to move to lower frequencies as the microphone was moved downstream. These features are similar to published high-Reynolds-number results.

SPL contours of the overall acoustic field were found to be similar in shape and level to both low- and high-Reynolds-number measurements. However, the low-Reynolds-number contours are displaced by approximately 6–10 jet diameters downstream. The displacement was attributed to the slower development of the overall flow-fluctuation amplitude in the low-Reynolds-number jet.

The results of acoustic measurements also indicate that two localized regions of major noise production are present in the acoustic field of the jet. This feature has been noted previously in a number of high-Reynolds-number investigations. It is also apparent that the angle with respect to the jet axis of the dominant noise radiation decreases with decreasing frequency. This result had also been noted by several investigators of high-Reynolds-number jet noise.

3.2. *Artificially excited jet*

3.2.1. *Effects of excitation.* In order to develop an understanding of the nature of the coherent fluctuations within the jet, an artificial disturbance was produced at the nozzle exit using a glow-discharge device. As discussed in an earlier paper (McLaughlin *et al.* 1975) the excitation device is similar to one used first by Kendall (1967). It consists of a tungsten electrode near the nozzle exit to which a 700 V peak-to-peak a.c. signal is applied with a 400 V negative bias. Because there is a breakdown voltage of approximately 600 V, this method actually introduces a small glow of ionized air which turns on and off at the excitation frequency. Such an excitation, in contrast to a sinusoidal excitation, possesses considerable harmonic content. However, the excitation is relatively weak as the energy input to the glow is only about 10^{-5} times the kinetic energy flux of the jet itself.

Figure 16 shows an example of the frequency spectra at several downstream locations in the centre of the shear layer, with the jet excited at $S = 0{\cdot}4$. The pass band of the spectrum analyser was set at 3 kHz ($\Delta S = 0{\cdot}05$) for these recordings. The spectra show that the the exciter generates a disturbance initially concentrated

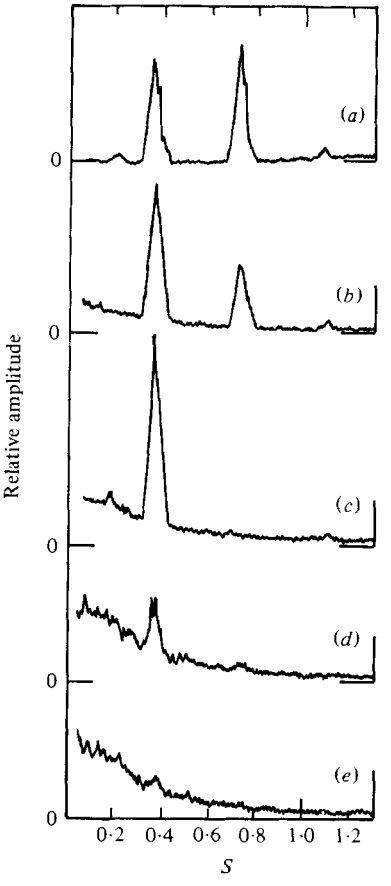

FIGURE 16. Hot-wire spectra in jet shear layer; jet excited at $S = 0{\cdot}4$. x/D: (*a*) 1; (*b*) 3; (*c*) 6; (*d*) 8; (*e*) 10.

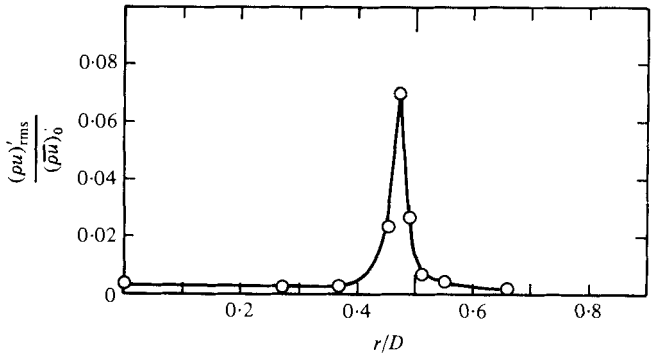

FIGURE 17. Radial profile of mass-velocity fluctuation amplitude. $x/D = 1$; jet excited at $S = 0{\cdot}2$.

at the fundamental forcing frequency and the second harmonic. Over the first six downstream diameters the amplitude of the fundamental grows slightly while the harmonic decays. Beyond $x/D = 6$ the fundamental rapidly decays until by $x/D = 10$ its presence is barely distinguishable. These spectra are typical of excitation spectra for frequencies over the range studied ($S = 0{\cdot}09$–$0{\cdot}8$), the only major difference

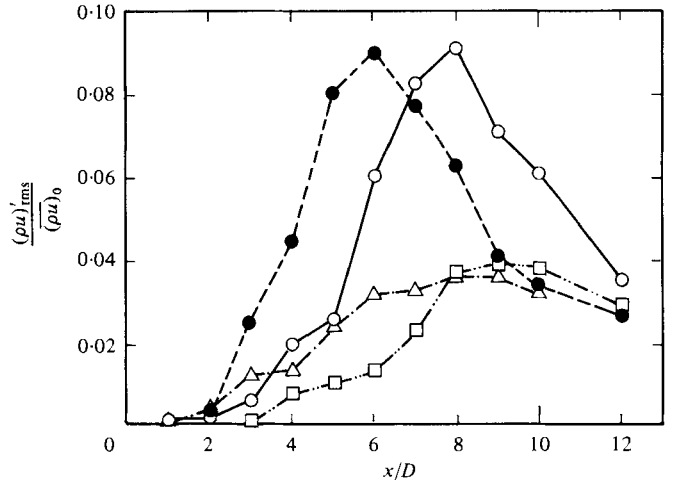

FIGURE 18. Band-passed mass-velocity fluctuation amplitude on the jet centre line. Excitation S: □, 0·1; ○, 0·2; ●, 0·4; △, 0·6.

being that at lower excitation frequencies more higher-harmonic content becomes apparent. Several previous investigators of free-shear flows (Browand 1966; Crow & Champagne 1971; Miksad 1972; Kibens 1979) have also found that artificial excitation causes the fluctuation spectra to become discretized in a similar manner.

Although the input disturbance from the exciter dominates the flow-fluctuation spectra near the nozzle, its effect is initially localized within the thin shear layer of the jet. This fact can be seen in figure 17, which shows a radial profile of the overall mass-velocity fluctuations at $x/D = 1$ for a jet excited at $S = 0{\cdot}2$. The measurements were made in the jet quadrant downstream of the exciter device. As a consequence of the excitation level the initial region of constant exponential growth (for a given spectral component) in the shear layer is partially bypassed.

The effect of the excitation on the jet centre-line mass-velocity fluctuations for four excitation frequencies is shown in figure 18. These measurements were band-pass filtered ± 1 kHz around the excitation frequency. An interesting result is evident from this figure. Apparently the jet core is much more responsive to excitation at the intermediate frequencies of $S = 0{\cdot}2$ and $S = 0{\cdot}4$. This result is closely analogous to results obtained by Crow & Champagne (1971) in a turbulent subsonic jet which was found to be most responsive to a $S = 0{\cdot}3$ excitation.

More recent subsonic-jet measurements by Chan (1974), Moore (1977) and Hussain & Zaman (1975) have also noted this selectivity. The exact mechanism by which the jet selects these frequencies is still poorly understood but it apparently exists in both subsonic and supersonic jets. Laufer & Monkewitz (1980) have proposed that the effect of downstream vortex pairing near the end of the potential core feeds upstream, modulating the instability and selecting the $S = 0{\cdot}3$ instability frequency. They have designed a series of experiments to explore this possibility in depth.

It is also important to determine the effect of the excitation on the mean flow as well as on the jet turbulent structure. Troutt (1978) presented mean-flow profiles which show that the development of the present jet occurs over a shorter distance

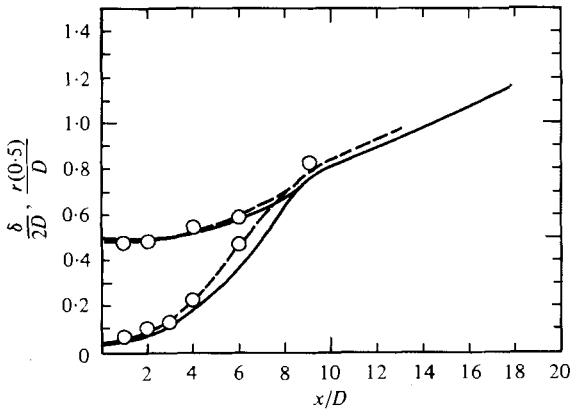

FIGURE 19. Axial distribution of mean-velocity-profile parameters. ——, natural jet; O----O, excited jet.

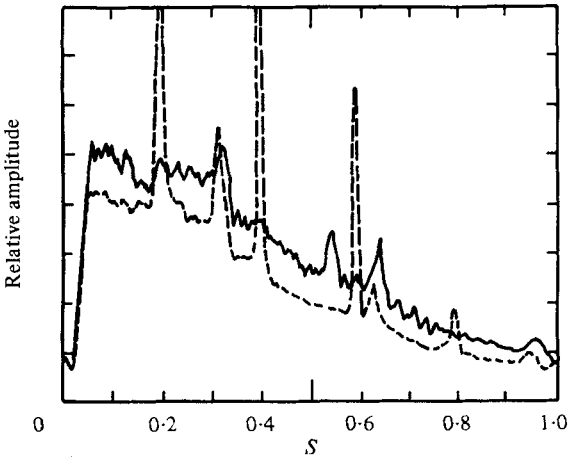

FIGURE 20. Frequency spectra of hot-wire signal with the probe positioned on the nozzle lip line at $x/D = 6$. ——, natural jet; ------, jet excited at $S = 0{\cdot}2$.

in the excited jet compared with the natural jet. Subsequent measurements have shown that the point excitation introduces a significant asymmetry in the mean-velocity profiles. This asymmetry decreases and is negligible by the end of the potential core. However, the spacially averaged jet flow does develop slightly faster in terms of downstream distance than the unexcited jet. As demonstrated earlier, the shear-layer thickness parameter δ is a more sensitive measure of the jet development than are the profiles. Therefore the parameters δ and $r(0{\cdot}5)$ corresponding to the excited and natural jets are presented in figure 19 to demonstrate the effect of excitation. In the excited-jet data the δ and $r(0{\cdot}5)$ parameters represent average values of measurements made on the top, bottom and two side shear layers. This figure indicates that the excited disturbances enhance the mean-flow development, a result which implies that naturally occurring organized large scales may also be efficient mixing agents.

It is instructive to examine more carefully hot-wire spectra from natural and excited jets. Figure 20 shows such spectra recorded with the probe positioned on the nozzle lip line at $x/D = 6$. At this position, the broad-band mass-velocity

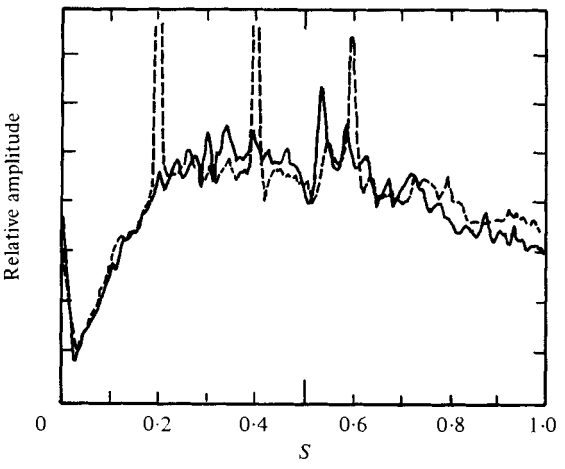

FIGURE 21. Acoustic spectra with microphone positioned in the maximum noise emission direction. ——, natural jet; - - - - -, jet excited at $S = 0{\cdot}2$.

fluctuations have saturated at their maximum value. The data show that the broad-band fluctuations are decreased by approximately 20% with the application of excitation at $S = 0{\cdot}2$. A similar result is obtained for excitation at $S = 0{\cdot}4$. For the recording shown in figure 20 the band pass of the spectrum analyser was set much narrower (300 Hz or $\Delta S = 0{\cdot}006$) than in the case of the measurements shown in figure 16. This shows that the response to excitation is amplified in only a very narrow band around the excitation frequency and its harmonics. The linear scale for the figure was chosen to maximize the resolution of the broad-band component. The level of the peak at the fundamental frequency is actually 10 times higher than the peak in the broad-band level and approximately 50% of the fluctuation energy is associated with the fluctuations at the excitation frequency and its harmonics. This spectral response including the broad-band suppression is similar to that reported by Crow & Champagne (1971) for an excited subsonic jet.

Like the flow fluctuations, the acoustic field responds strongly at the excitation frequency and its harmonics when excitation is applied to the jet. Figure 21 shows microphone spectra measured for the natural jet and for the jet excited at the fundamental frequency of $S = 0{\cdot}2$. The microphone is located in the acoustic field at an angle of 30° from the jet axis. As in the hot-wire data presented in figure 20 approximately 50% of the energy is associated with the fundamental excitation frequency and its harmonics. However, contrary to the hot-wire spectra, no significant change is evident in the broad-band noise. This is in contrast to the subsonic-jet experiments of Bechert & Pfizenmaier (1975) and Moore (1977), who measured an enhancement of the broad-band component of noise with the application of excitation near $S = 0{\cdot}3$. Excitation at frequencies above $S = 0{\cdot}6$ yielded suppression of the broad-band radiated noise to the extent that the overall SPL in the maximum-noise-emission direction decreased by as much as 3 dB. This suppression of broad-band radiated noise by excitation at relatively high frequencies was also observed in subsonic jets by Kibens (1979).

3.2.2. *Excited-flow fluctuation measurements.* Measurements of the axial wavelength of excited disturbances in the jet were made by cross-correlating the hot-wire

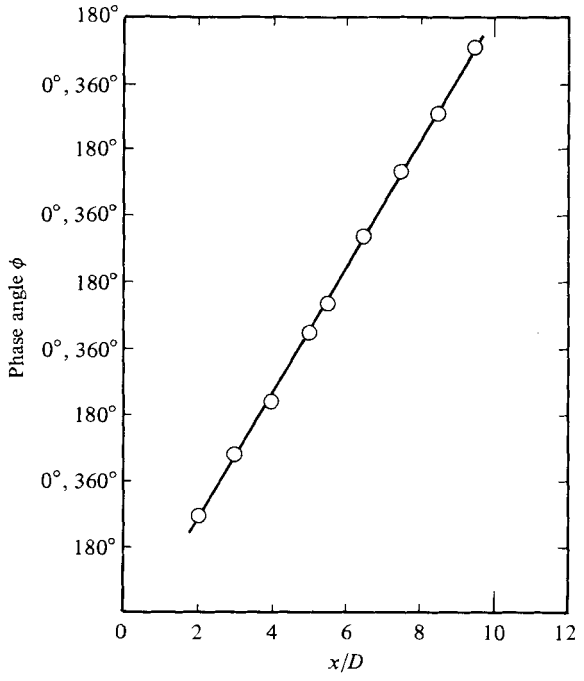

FIGURE 22. Flow-disturbance phase angle; jet excited at $S = 0{\cdot}4$.

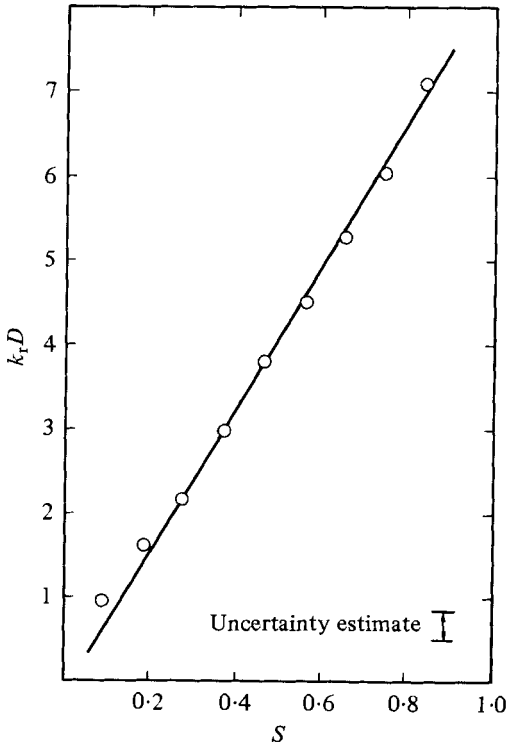

FIGURE 23. Axial wavenumber of excited disturbance. ○, present experiment; ——, Tam (1972) prediction.

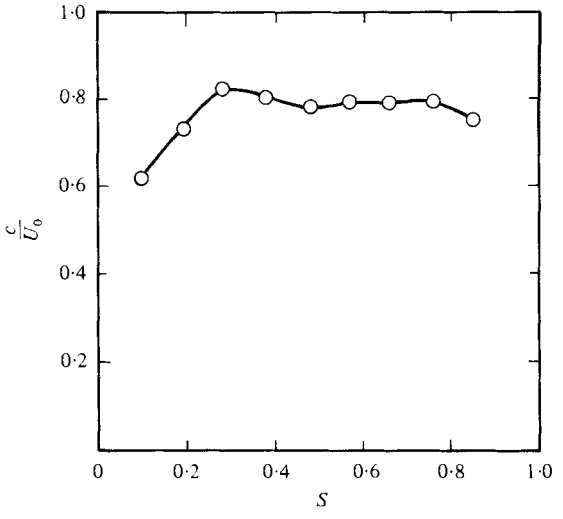

FIGURE 24. Axial phase velocity of excited disturbance.

signal with the excitation signal and measuring the change in the time lag of the peak of the correlation curves for various downstream positions. An example of these measurements for a typical disturbance is shown in figure 22. The results of the wavelength measurements, presented in terms of non-dimensional wavenumber $k_r D$ as a function of excitation Strouhal number, are shown in figure 23. The solid line shown on the figure is a prediction of the eigenvalue relation from Tam's (1972) theory.† Needless to say the agreement between theory and experiment is remarkable. This is especially so when one considers that Tam used a simple parallel mean flow with an infinitesimal shear-layer thickness as an input.

Multiplying the axial wavelength by the frequency of the disturbance gives the axial phase velocity of the disturbance. Figure 24 shows the axial phase velocity as a function of Strouhal number. For most of the Strouhal-number range the phase velocity is approximately constant; however, it decreases considerably at the low-frequency end of the spectrum. This trend for low-frequency disturbances was also noted by Chan (1974) for azimuthal modes $n = 1$ and $n = 2$ in a subsonic jet. It is also notable that the average convection velocity for disturbances between $S = 0{\cdot}3$ and $S = 0{\cdot}8$ is approximately $0{\cdot}80U_0$, which is in close agreement with the value measured by Dutt (1977) from laser–schlieren cross-correlations in a high-Reynolds-number, $M = 2{\cdot}0$ jet.

An important point to note in addition is that disturbances travelling faster than $0{\cdot}65U_0$ will possess an axial phase velocity which is supersonic with respect to the air outside the jet. Supersonically travelling waves have the ability to radiate Mach-wave-like sound emission (Phillips 1960; Ffowcs Williams 1963). Morrison & McLaughlin (1979) have shown that the noise radiation has different propagating characteristics when the phase velocity of the instability waves exceeds the ambient acoustic velocity.

Morris & Tam (1977) claim that only waves with supersonic axial phase velocities

† It should be noted here that Troutt (1978) made a slight error in calculating and presenting Tam's eigenvalue relation.

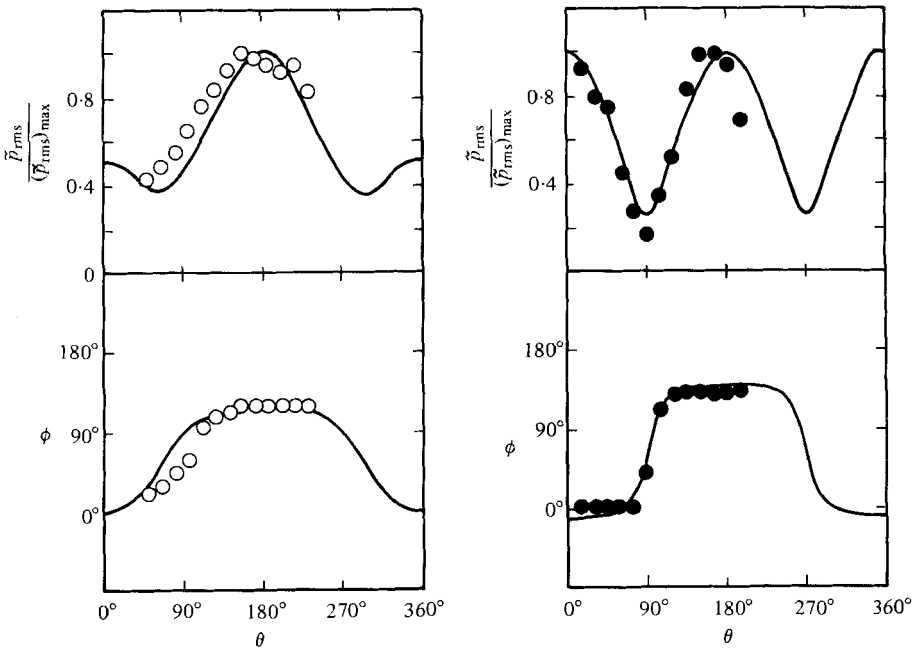

FIGURE 25. Coherent sound-pressure-fluctuation amplitude and phase angle as a function of azimuthal angle. ○, ●, experimental data, ——, numerical curve fit. S component: ○, 0·2; ●, 0·4.

will radiate to the far field. The instability waves in the $M = 1{\cdot}4$ and 2·1 jets at low Reynolds number studied by Morrison & McLaughlin (1980) travel subsonically (with respect to the surrounding air) but they nevertheless radiate efficiently to the far field. Morris & Tam (1977), Liu (1974) and Tam (1971) believe that because the waves grow and decay spacially they actually possess supersonic phase components. Morris & Tam (1979, personal communication) have pointed out that this is one area of the instability-analysis noise-generation model which needs and is receiving attention.

Azimuthal dependence of disturbances. Since Tam (1972) assumed an $n = \pm 1$ mode shape for his theory it was important to check the experimental-disturbance azimuthal character. This was done by measuring the change in the correlation phase between the hot-wire and exciter signals as a function of θ. An axial position of $x/D = 4$ was used for Strouhal numbers of 0·2 and 0·4. For both frequencies the $n = \pm 1$ modes appeared dominant. However, due to probe-resolution problems combined with the radial complexity of the phase of the disturbance, the data did not have enough certainty to delineate the exact percentages of mode components.

A reasonably accurate delineation of the azimuthal-modal content of the disturbance was determined by measuring the relative phase between the exciter signal and the microphone located at various azimuthal angles in the near field. The microphone was located just outside the flow field on a cylindrical radius of $r/D = 3$ at an axial location $x/D = 12$ and the amplitude of the phase-averaged signal was also recorded for each measurement position. Implicit in this measurement is the assumption that the azimuthal-modal content of the near acoustic field will be representative of the flow-fluctuation content. A similar assumption was made previously in a study by Petersen (1978) on the modal distribution in a subsonic

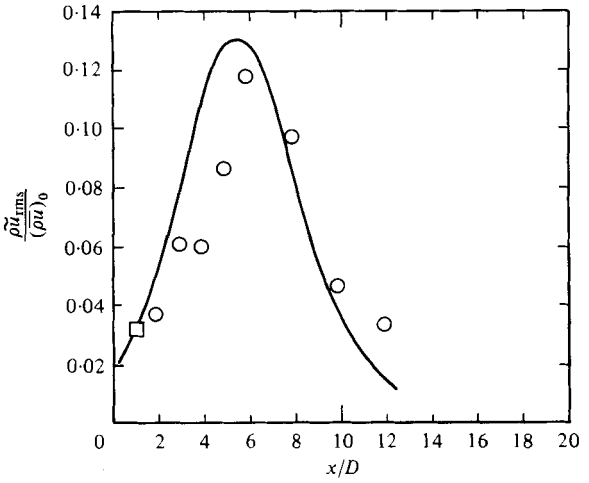

FIGURE 26. Coherent mass-velocity-fluctuation amplitude in jet shear layer (S = 0·2 component). ○, present experiment; ——, Tester *et al.* (1978) prediction.

jet. The results of the measurements for the S = 0·2 and 0·4 components are shown in figure 25. The amplitude measurements are non-dimensionalized by the amplitude of maximum phase-averaged signal on the arc. These azimuthal acoustic measurements were found to have much less apparent scatter than the azimuthal flow measurements. This can be attributed to the fact that the near acoustic field has much less radial dependence than the flow field; consequently reducing probe-resolution problems.

Numerical fits to the data were obtained by superposing three azimuthal modes $n = 0, +1, -1$. These modes are represented mathematically by the equation

$$q_n = A_n \exp\left[i(n\theta - \omega t + \alpha_n)\right] \quad (n = 0, +1, -1),$$

where α_n represents a possible phase difference between modes at the measurement position. Before attempting to find A_n and α_n for each mode it was assumed that $A_1 = A_{-1}$ and that $\alpha_1 = \alpha_{-1}$. Since the mean flow was found to be reasonably axisymmetric by this downstream position, α_1 and α_{-1} can be referenced to any value. For simplicity $\alpha_{\pm 1} = 0$ was chosen. The best fits for the data were found to be $A_0/A_1 = 1{\cdot}4$, with $\alpha_0 = 130°$ for the S = 0·2 disturbance, and $A_0/A_1 = 0{\cdot}5$ with $\alpha_0 = 90°$ for the S = 0·4 data.

It is of interest to note that the antisymmetric excitation device is apparently capable of exciting both antisymmetric and axisymmetric flow disturbances. This finding indicates that the excitation device does not necessarily dictate the downstream character of the artificial disturbance.

Coherent wave evolution. In our discussion of the data of figure 10, it was noted that the band-passed flow-fluctuation measurements did not display the rapid axial decay predicted by the Morris–Tam instability analysis. Artificial excitation of specific spectral components of the jet disturbances allows us to determine the coherent portion of the flow fluctuations and hence possibly represent more accurately the quantity predicted by the analysis. Figure 26 shows the axial development of the coherent portion of the mass-velocity fluctuations measured on the nozzle lip line for the S = 0·2 disturbance. The experimental data are compared with the

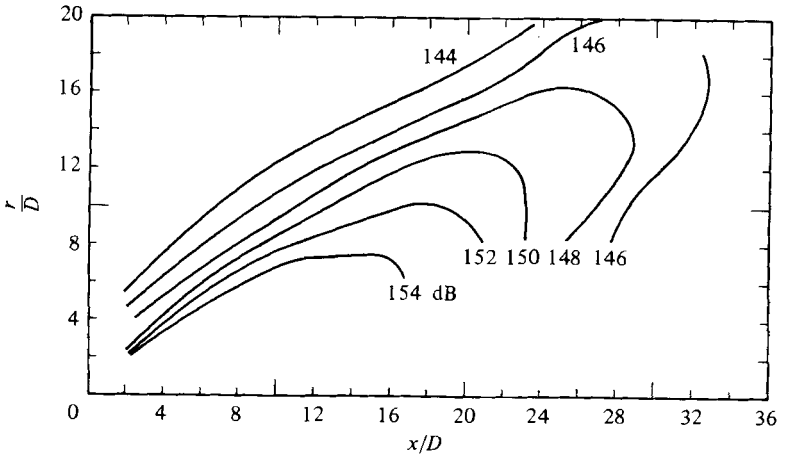

FIGURE 27. Overall sound-pressure level contours; jet excited at $S = 0{\cdot}2$.

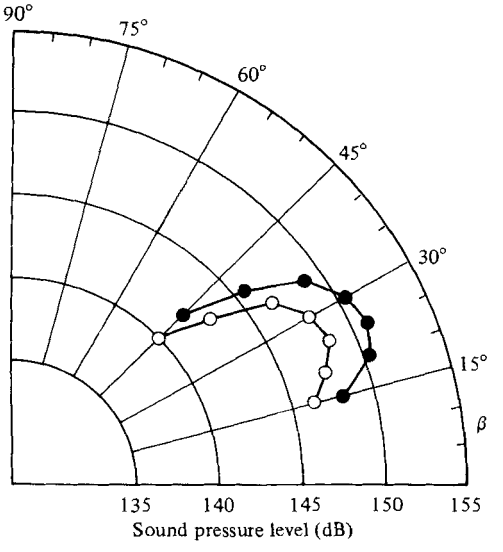

FIGURE 28. Overall sound-pressure level directivity; $R/D = 24$.
○, natural jet; ●, excited jet.

calculation using the Morris–Tam algorithm as documented in Tester *et al.* (1978). The mean-flow profiles input into the calculation correspond to the spacially averaged mean flow as presented earlier in figure 19. Also the prediction represents a combination of $n = 0$ and $n = \pm 1$ modes using the proportion at the crest of $A_0/A_1 = 1{\cdot}4$ as was determined from the near-field microphone measurements of figure 25. The levels of the experimental and calculated data were matched at $x/D = 1$, as was done with the earlier wave evolution comparisons of figure 10.

A stringently accurate comparison would necessitate establishing the mode ratio at every axial location in the jet. As explained earlier, this was not practical because of insurmountable probe-resolution problems. Nevertheless, the very good agreement between the experimental data and the calculation as performed suggests that the Morris–Tam analysis has considerable merit. The data of figures 10 and 26 demon-

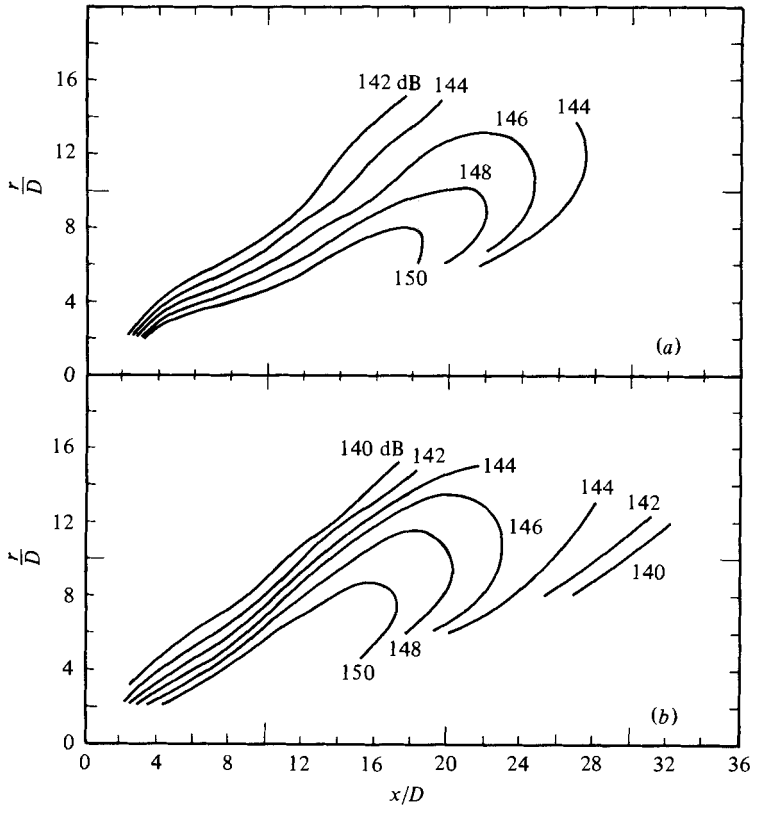

FIGURE 29. Band-passed sound-pressure level contours for excited jet. (*a*) S = 0·15–0·23, excited at S = 0·2; (*b*) S = 0·30–0·45, excited at S = 0·4.

strate quite convincingly that the instability calculation models the coherent portion of the spectral components rather than the total fluctuation level within a specific band pass.

3.2.3. *Acoustic radiation from artificially excited jet.* SPL contours of the overall near field for the jet excited at S = 0·2 are shown in figure 27. The shapes and positions of these contours are approximately the same as the natural-jet contours shown in figure 11. However, an increase in the noise level at corresponding locations in the acoustic field is apparent. A directivity plot generated from these contours is shown in figure 28. For comparison, the natural-jet measurements are shown on the plot. This plot shows that the directivity of the noise radiation in the two cases is almost identical, although the amplitude is approximately 2–3 dB higher in the excited-jet case.

SPL contours filtered around the fundamental excitation frequency are shown in figure 29 for the S = 0·2 and 0·4 components. The contours are similar in overall shape to the unexcited-jet data (figure 15), especially in the downstream lobed region. The upstream bulge region present in the unexcited-jet data (figure 15), however, is noticeably diminished. This result suggests that the noise from coherent disturbances tends to propagate predominantly in the downstream direction.

Directivity patterns of the noise in the downstream region for both excited and natural cases are shown in figure 30. As would be expected, as a result of the

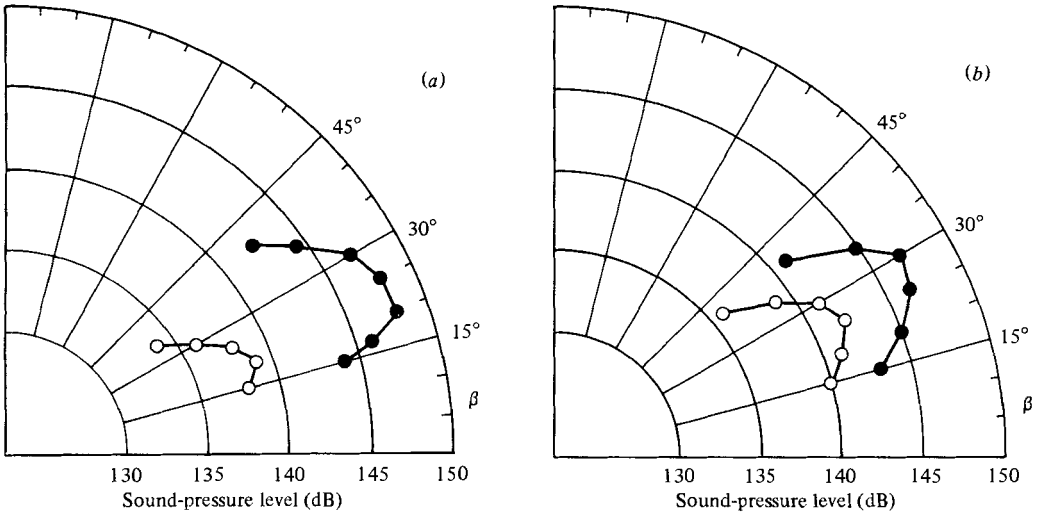

FIGURE 30. Band-passed sound-pressure level directivity plots. ○, natural jet; ●, excited jet. Excitation S: (*a*) 0·2; (*b*) 0·4.

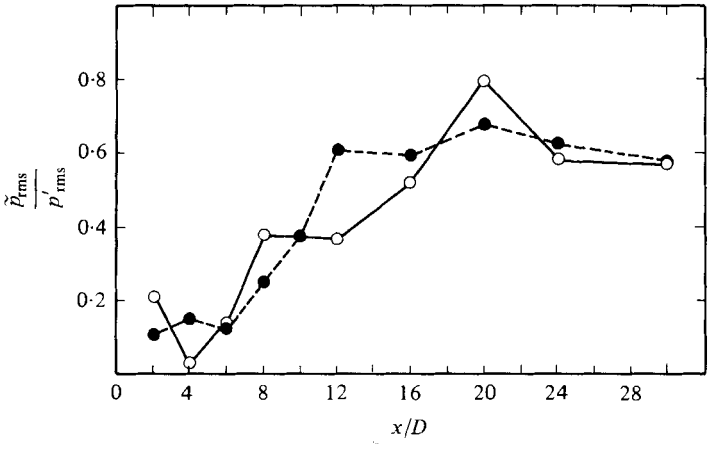

FIGURE 31. Coherent sound-pressure level; r/D = 8. S component: ○, 0·2; ●, 0·4.

concentrated nature of the excited acoustic spectra, there is a considerable increase in the SPL with excitation for a given angle. Surprisingly, however, there seems to be very little change in the directivity of the noise radiation between the natural and excited jets. This result also implies that the artificial disturbances may well generate noise by the same mechanism responsible for the downstream noise-emission pattern in the natural jet.

By phase-averaging the microphone signal in the noise-radiation field, the fraction of the total signal caused directly by the excited-flow disturbances was determined. Figure 31 shows the percentage of the phase-averaged component as a function of downstream position for two excitation frequencies (S = 0·2 and 0·4). These measurements were recorded with the microphone at a constant radial location of 8 diameters. At low values of x/D, the noise at both Strouhal numbers shows a low percentage of the phase-averaged (coherent) component. However, as downstream

S	$\frac{\lambda_r}{D}$	α	$\frac{c_a}{a_0}$	$\frac{\lambda_I}{D}$	$\frac{c}{a_0}$	μ
0·2	3·23	48°	0·94	3·85	1·12	63°
0·4	1·74	56°	0·99	2·11	1·24	54°

TABLE 1. Results of acoustic-field phase measurements

position is increased both frequencies begin to show an increase in the phase-averaged component. The phase-averaged portion of the $S = 0{\cdot}4$ disturbance goes above 50 % by $x/D = 11$, while the coherent portion of the $S = 0{\cdot}2$ reaches this value slightly farther downstream at $x/D = 16$. These points correspond approximately to the location of the inflection region in the filtered natural-jet contours (figure 15), indicating the beginning of the downstream lobed area. At the maximum-noise-emission direction the coherent portion of the radiated noise increases further, and actually reaches 80 % of the total radiated noise for the $S = 0{\cdot}2$ component at $x/D = 20$ and $r/D = 8$.

Several investigators of high-speed jets (Dutt 1977; Dahan & Elias 1976; Maestrello 1976) have also measured high correlations for the noise at small spherical angles to the jet axis. However, for their experiments, the jets were not artificially excited and the coherence levels were considerably lower than the present results. It is our belief that the organized disturbances created by the exciter are instantaneously similar to naturally occurring flow fluctuations. For the natural jet the organized disturbances, however, possess considerable levels of phase jitter, which reduce the long-time average coherency levels.

The high percentages of coherent-noise levels for the present excited jet constitute evidence that the large-scale coherent structure in the jet radiates *directly* to the acoustic field, and in fact produces the dominant noise radiation. This result is extremely important as it is one of the few cases of unrefutable experimental evidence of the powerful noise-radiating capability of jet large-scale structure. Of course a point which is open to conjecture is whether or not such noise-radiation processes carry over to the natural jet. The many similarities between the radiated noise in the natural- and excited-jet cases (figures 15, 28, 29 and 30) provide evidence supporting such a point of view.

Phase-front orientation measurements in the acoustic field provide valuable information on the generation and propagation characteristics of the radiated noise. These measurements have been performed in the near field of the jet excited at $S = 0{\cdot}2$ and at $S = 0{\cdot}4$ by cross-correlating the microphone and exciter signals and measuring the change in time lag for various microphone positions. Table 1 shows the results of these measurements for the two frequencies. λ_a is the measured wavelength in the near field and α is the angle the phase front makes with the axis; both results correspond to the region of the highest-amplitude near-field sound. The ratio c_a/a_0 represents the phase velocity computed from the wavelength λ_a and frequency of the wave, non-dimensionalized with the ambient acoustic velocity. If c_a/a_0 is equal to 1 (within experimental uncertainty) then we can conclude that the measured pressure fluctuations are primarily radiating noise. Such is the case in the $S = 0{\cdot}4$ frequency component. The value of $c_a/a_0 = 0{\cdot}94$ for the $S = 0{\cdot}2$ components suggests that within the region of measurement (the microphone is in

the near field) some of the pressure fluctuations are hydrodynamic (non-radiating) in nature.

Included in table 1 are the results of the wavelength measurements performed in the flow field with the hot-wire probe (λ_f). From the disturbance wavelength and frequency a phase velocity c was calculated as discussed in §3.2.2. The Mach angle μ associated with the flow-disturbance phase velocity is also given in table 1. It is interesting to note that the measured phase front angle and the calculated Mach wave angle are equal (within experimental uncertainty) for the $S = 0{\cdot}4$ component. The $S = 0{\cdot}2$ component does not appear to radiate in a Mach-value fashion, as the phase fronts are inclined at an angle considerably lower than the Mach angle. This type of radiation was observed by Morrison & McLaughlin (1979) in low-Reynolds-number supersonic-jet measurements for instability waves travelling just above and below the speed of sound.

Based on these results and Morrison & McLaughlin's measurements, it seems that a simple eddy–Mach-wave model for the major noise generation mechanism is not of sufficient complexity to explain all of the measured noise-field properties. However, it does appear that a Mach-wave component of noise radiation does occur for higher-frequency and consequently higher-phase-velocity disturbances.

Mach-wave-type radiation has been noticed by other experimenters using flow-visualization techniques (Salant 1973; Lowson & Ollerhead 1968). Recently Dutt (1977) found that the angle of the Mach waves in his shadowgraphs implied a disturbance convection velocity which was in agreement with laser cross-correlation measurements made on the edge of the flow field.

The acoustic phase-front measurements can also be used in conjunction with the SPL contours (figure 29) with a simple ray-tracing technique for the purpose of determining regions in the jet of apparent strong noise production. This technique indicates that the dominant noise production for the $S = 0{\cdot}2$ noise component is centred at approximately $x/D = 10$, while the $S = 0{\cdot}4$ component sources are centred at about $x/D = 6$.

Flow-fluctuation amplitude measurements have shown that both of these locations are downstream of the initial growth of the flow disturbances, and in the axial region where the disturbance saturates and begins to decay. In fact, the determined locations coincide very closely with the axial location where the coherent portion of the flow fluctuations begins to decay rapidly. This finding appears to support theoretical studies of Merkine & Liu (1975) in which they attribute a strong noise-generation mechanism to the nonlinear disintegration of the coherent disturbance. Again it is emphasized that the data indicate that the large-scale coherent structure itself is a *direct* noise radiator through the disintegration process. Finally, it is important to note that the axial location of the apparent noise sources determined with the present technique are in reasonable agreement with the noise source location measurements performed by Laufer *et al.* (1976) using a directional-microphone system.

3.2.4. *Summary of excited-jet results.* It was found that the artificial exciter generates a flow disturbance at the fundamental frequency and its higher harmonics. For several diameters downstream of the nozzle exit, it was observed that the flow-fluctuation spectral content in the jet shear layer was concentrated at the excitation frequency and its harmonics. Further downstream, the spectral content

of the flow fluctuations disperses, so that at $x/D = 10$ the effect due to the excitation is not apparent in the spectra. Centre-line flow-fluctuation measurements demonstrated that the jet core is most responsive to excitation at the Strouhal numbers close to $S = 0{\cdot}3$. Also, excitation at $S = 0{\cdot}2$ was shown to increase slightly the mean-flow spreading rate of the jet.

Hot-wire measurements of the excited disturbances demonstrate that the variation of wavelength with Strouhal number is in excellent agreement with Tam's (1972) linear stability theory. The axial phase velocity calculated from the measured wavelengths shows an increase at low Strouhal numbers. Above $S = 0{\cdot}4$ up to $S = 0{\cdot}8$, the convection velocity remains approximately constant at $0{\cdot}80U_0$.

Phase-averaged amplitude measurements of excited flow fluctuations in the jet shear layer show that the overall development of the $S = 0{\cdot}2$ disturbance is in general agreement with theoretical stability predictions using the method of Morris & Tam (1977).

Near-field microphone measurements performed just outside the flow field provided estimates of the azimuthal content of the $S = 0{\cdot}2$ and $0{\cdot}4$ components of the jet fluctuations. The $n = \pm 1$ mode dominates the $S = 0{\cdot}4$ fluctuations, while the $S = 0{\cdot}2$ component contains a substantial axisymmetric ($n = 0$) component along with the $n = \pm 1$ modes. Hot-wire measurements in the flow field are in general agreement with this; however, the accuracy of the hot-wire measurements was not precise enough to obtain the proportions of $n = 0$ and $n = \pm 1$ modes.

Noise-amplitude measurements indicate that a large portion of the noise from the excited disturbances propagates toward the downstream lobed region of the contours. Phase-averaged acoustic measurements confirm this fact. They also confirmed the fact that the large-scale coherent structure is a powerful and direct radiator of noise to the far field.

The directivity of the noise from the excited disturbances was also found to be almost identical with the natural case for the two Strouhal numbers observed ($S = 0{\cdot}2$ and $0{\cdot}4$). This measurement indicates that the natural and excited disturbances radiate noise in the downstream direction by a similar mechanism. Assuming this to be true, these measurements support the thesis that organized flow disturbances are directly responsible for a major portion of the downstream noise radiation produced by supersonic jets.

Wave-front acoustic-orientation measurements indicate that the higher spectral component studied ($S = 0{\cdot}4$) radiates noise in a manner similar to eddy–Mach-wave propagation models. The lower-frequency wave ($S = 0{\cdot}2$), however, did not appear to radiate noise in this manner, indicating the possibility of other types of noise-generation mechanisms. A simple ray-tracing technique indicated that the major noise-source locations occur where the waves saturate and begin to decay rapidly.

4. Concluding remarks

Interpretations of natural jet phenomena based on the artificially excited results of this study should be made with care. Since it was shown that excitation not only causes dramatic changes in the initial flow-fluctuation spectra, but can also cause changes in the mean-flow development, the precise relationship between the artificially excited flow and the natural jet are debatable. However, it does not

seem unreasonable to expect that measured properties of the excited disturbances such as wavelength, interaction with the core flow, and noise-generation mechanics are also characteristic of naturally occurring large-scale organized disturbances. This type of assumption has been used by previous investigators in flows of this type and its application is favoured by the authors of the present study.

Taking this point of view, several important conclusions can be drawn from these measurements. The growth rates of the initial jet instabilities and the wavelengths of the coherent disturbances are in excellent agreement with linear-stability-theory predictions over a broad frequency range. The measured overall evolution of the coherent-wave amplitude at two frequencies (S = 0·2 and 0·4) is also in general agreement with the recent quasi-linear instability theory developed by Morris & Tam (1977).

Measurements performed in the acoustic field demonstrate that organized disturbances are powerful *direct* noise producers. The correspondence of maximum noise-emission directivity between natural and excited jets supports the thesis that large-scale coherent structures are dominant noise producers in conventional high-Reynolds-number supersonic jets.

Another interesting result obtained in this study was the finding that artificial disturbances near S = 0·3 were able to affect the jet core much more efficiently than higher and lower frequencies. This result is quite similar to the result first noted by Crow & Champagne (1971) in a study of a subsonic jet, and later observed by other experimentalists for subsonic jets. This finding indicates that the supersonic jet has a frequency-selection mechanism which is outside the scope of linear stability theory, as Crow & Champagne previously observed for the subsonic jet. Unfortunately, the nature of this selection mechanism is still poorly understood. A series of experiments recently conducted and currently underway by Laufer & Monkewitz (1980) will, it is hoped, explore a possible feedback mechanism involved in selecting the preferred spectral mode of the subsonic jet.

The areas of agreement between experiment and instability theory, together with the present absence of an adequate prediction method for the apparent frequency-selection phenomenon of axisymmetric jets, support the need for continued development of instability analyses for both subsonic and supersonic jet flows.

This research was supported by the National Science Foundation under Grant no. ENG 75-21405, and the National Aeronautics and Space Administration under Grant no. NSG 1467. The suggestions and assistance of Mr T. F. Hu, Dr G. L. Morrison, Dr J. M. Seiner, Mr J. L. Stromberg, Mr J. D. Swearingen and Dr W. G. Tiederman are gratefully acknowledged.

REFERENCES

Bechert, D. & Pfizenmaier, E. 1975 On the amplification of broad band jet noise by pure tone excitation. *J. Sound Vib.* **43**, 581–587.

Bishop, K. A., Ffowcs Williams, J. E. & Smith, W. 1971 On the noise sources of the unsuppressed high-speed jet. *J. Fluid Mech.* **50**, 21–31.

Browand, F. K. 1966 An experimental investigation of the instability of an incompressible, separated shear layer. *J. Fluid Mech.* **26**, 281–307.

Chan, Y. Y. 1974 Spatial waves in turbulent jets. *Phys. Fluids* **17**, 46–53.

CRIGHTON, D. G. & GASTER, M. 1976 Stability of slowly diverging jet flow. *J. Fluid Mech.* **77**, 397–413.

CROW, S. C. & CHAMPAGNE, F. H. 1971 Orderly structure in jet turbulence. *J. Fluid Mech.* **48**, 547–591.

DAHAN, P. C. & ÉLIAS, G. 1976 Source structure pattern in a hot jet by infrared–microphone correlation. *A.I.A.A. Paper* no. 76–542.

DOSANJH, D. S. & YU, J. C. 1968 Noise from underexpanded axisymmetric jet flow using radial jet flow impingement. In *Proc. A.F.O.S.R.-U.T.I.A.S. Symp. on Aerodynamic Noise, Toronto*, pp. 169–188.

DUTT, B. 1977 Role of large scale structures in the noise generation of a turbulent supersonic jet. Ph.D. dissertation, University of Southern California.

FFOWCS WILLIAMS, J. E. 1963 The noise from turbulence convected at high speed. *Phil. Trans. R. Soc. Lond.* A **255**, 459–503.

HUSSAIN, A. K. M. F. & ZAMAN, K. B. M. Q. 1975 Effect of acoustic excitation on the turbulent structure of a circular jet. In *Proc. 3rd Interagency Symp. on University Research in Transportation Noise, University of Utah, Salt Lake City.*

JOHNSON, C. B. & BONEY, L. R. 1975 A method for calculating a real-gas two-dimensional nozzle contour including the effects of gamma. *N.A.S.A. TM* X-3243, Langley Research Center, Hampton, Virginia.

KENDALL, J. M. 1967 Supersonic boundary layer stability experiments. In *Proc. Boundary Layer Trans. Study Group, Meeting*, II (*Aerospace Rep.* TR-0158 (S3816-63)-1).

KIBENS, V. 1979 Discrete noise spectrum generated by an acoustically excited jet. *A.I.A.A. Paper* no. 79-0592.

KO, C. L., MCLAUGHLIN, D. K. & TROUTT, T. R. 1978 Supersonic hot-wire fluctuation data analysis with a conduction end-loss correction. *J. Phys.* E, *Sci. Instrum.* **11**, 488–494.

LAU, J. C., FISHER, M. J. & FUCHS, H. V. 1972 The intrinsic structure of turbulent jets. *J. Sound Vib.* **22**, 379–406.

LAUFER, J., KAPLAN, R. E. & CHU, W. T. 1973 Acoustic modeling of the jet noise abatement problem. In *Proc. Interagency Symp.* on *University Research in Transportation Noise, Stanford, California.*

LAUFER, J. & MONKEWITZ, P. 1980 On turbulent jet flows: a new perspective. *A.I.A.A. Paper* no. 80-0962.

LAUFER, J., SCHLINKER, R. S. & KAPLAN, R. E. 1976 Experiments on supersonic jet noise. *A.I.A.A. J.* **14**, 489–497.

LIU, J. T. C. 1974 Developing large-scale wavelike eddies and the near jet noise field. *J. Fluid Mech.* **62**, 437–464.

LOWSON, M. V. & OLLERHEAD, J. B. 1968 Visualization of noise from cold supersonic jets. *J. Acoust. Soc. Am.* **44**, 624–000.

MAESTRELLO, L. 1976 Two point correlation of sound pressure in the far field of a jet: Experiment. *N.A.S.A. TM*-72835.

MCLAUGHLIN, D. K., MORRISON, G. L. & TROUTT, T. R. 1975 Experiments on the instability waves in a supersonic jet and their acoustic radiation. *J. Fluid Mech.* **69**, 73–95.

MCLAUGHLIN, D. K., MORRISON, G. L. & TROUTT, T. R. 1977 Reynolds number dependence in supersonic jet noise. *A.I.A.A. J.* **15**, 526–532.

MCLAUGHLIN, D. K., SEINER, J. M. & LIU, C. H. 1980 On noise generated by large scale instabilities in supersonic jets. *A.I.A.A. Paper* no. 80-0964.

MERKINE, L. O. & LIU, T. T. C. 1975 On the development of noise-producing larger-scale wavelike eddies in a plane turbulent jet. *J. Fluid Mech.* **70**, 353–368.

MICHALKE, A. 1969 Sound generation by amplified disturbances in free shear layers. *Deutsche Luft- und Raumfahrt Rep.* no. 69–90.

MICHALKE, A. 1971 Instibilität eines kompressiblen runden Freistrahls unter Beruchksichtigung des Einflusses der Strahlgrenzschichtdicke. *Z. Flugwiss.* **19**, 319–328.

MIKSAD, R. W. 1972 Experiments on the nonlinear states of free-shear-layer transition. *J. Fluid Mech.* **56**, 695–719.

MOLLO-CHRISTENSEN, E. 1960 Some aspects of free shear-layer instability and sound emission. *N.A.T.O. Rep.* no. 260.

MOLLO-CHRISTENSEN, E. 1967 Jet noise and shear flow instability seen from an experimenter's viewpoint. *J. Appl. Mech.* **34**, 1–7.

MOORE, C. J. 1977 The role of shear-layer instability waves in jet exhaust noise. *J. Fluid Mech.* **80**, 321–357.

MORRIS, P. J. 1977 Flow characteristics of the large scale wavelike structure of a supersonic round jet. *J. Sound Vib.* **53**, 223–244.

MORRIS, P. J. & TAM, C. K. W. 1977 Near and far field noise from large-scale instabilities of axisymmetric jets. *A.I.A.A. Paper* no. 77–1351.

MORRISON, G. L. 1977 Flow instability and acoustic radiation measurements of low Reynolds number supersonic jets. Ph.D. dissertation, Oklahoma State University, Stillwater, Oklahoma.

MORRISON, G. L. & MCLAUGHLIN, D. K. 1979 The noise generation by instabilities in low Reynolds number supersonic jets. *J. Sound Vib.* **65**, 177–191.

MORRISON, G. L. & MCLAUGHLIN, D. K. 1980 Instability process in low Reynolds number supersonic jets. *A.I.A.A. J.* **18**, 793–800.

PETERSEN, R. A. 1978 Influence of wave dispersion on vortex pairing in a jet. *J. Fluid Mech.* **89**, 469–495.

PHILLIPS, O. M. 1960 On the generation of sound by supersonic turbulent shear layers. *J. Fluid Mech.* **9**, 1–28.

POTTER, R. C. 1968 An investigation to locate the acoustic sources in a high speed jet exhaust stream. *Wyle Lab. Tech. Rep.* WR 68-4.

ROSE, W. C. 1973 The behavior of a compressible turbulent boundary layer in a shock-wave-induced adverse pressure gradient. *N.A.S.A. TN* D-7092.

SALANT, R. F. 1973 Investigation of jet noise using optical holography. *Dept of Transportation Rep.* no. DOT-TSC-OST-73-11.

SEDEL'NIKOV, T. K. 1967 The frequency spectrum of the noise of a supersonic jet. *Phys. Aero. Noise.* Moscow: Nauka. (Trans. *N.A.S.A. TTF*-538, 1969, pp. 71–75.)

STROMBERG, J. L., MCLAUGHLIN, D. K. & TROUTT, T. R. 1979 Flowfield and acoustic properties of a Mach number 0·9 jet at a low Reynolds number. *A.I.A.A. Paper* no. 79-0593.

TAM, C. K. W. 1971 Directional acoustic radiation from a supersonic jet generated by shear layer instability. *J. Fluid Mech.* **46**, 757–768.

TAM, C. K. W. 1972 On the noise of a nearly ideally expanded supersonic jet. *J. Fluid Mech.* **51**, 69–95.

TAM, C. K. W. 1975 Supersonic jet noise generated by large scale disturbances. *J. Sound Vib.* **38**, 51–79.

TESTER, B. J., MORRIS, P. J., LAU, J. C. & TANNA, H. K. 1978 The generation, radiation and prediction of supersonic jet noise, 1. *Tech. Rep.* AFAPL-TR-78-85.

TROUTT, T. R. 1978 Measurements on the flow and acoustic properties of a moderate Reynolds number supersonic jet. Ph.D. dissertation, Oklahoma State University, Stillwater, Oklahoma.

YU, J. C. & DOSANJH, D. S. 1972 Noise field of supersonic Mach 1·5 cold model jet. *J. Acoust. Soc. Am.* **51**, 1400–1410.